

The Interaction of HIV-1 Inhibitor 3,3',3'',3'''-Ethylenetetraakis-4-Hydroxycoumarin with Bovine Serum Albumin at Different pH

Sheying Dong,* Zhuqing Yu, Zhiqin Li, and Tinglin Huang†

College of Sciences, Xian University of Architecture and Technology, Xian 710055, China

*E-mail: dshiney2004@yahoo.com.cn

†College of Environmental and Municipal Engineering, Xian University of Architecture and Technology, Xian 71005, China

Received February 16, 2011, Accepted May 3, 2011

We studied the interaction of 3,3',3'',3'''-ethylenetetraakis-4-hydroxycoumarin (EHC) with bovine serum albumin (BSA) in acetate buffer and phosphate buffer with different pH values by UV-vis absorption spectrometry and fluorescence spectrometry respectively. It was found that the pH values of the buffer solutions had an effect on the interaction process. In acetate buffer of pH 4.70, the carbonyl groups in EHC bound to the amino groups in BSA by means of hydrogen bond and van der Waals force, which made the extent of peptide chain in BSA changed. By contrast, in phosphate buffer of pH 7.40, hydrophobic force played a major role in the interaction between EHC and BSA, while the hydrogen bond and van der Waals force were also involved in the interaction. The results of spectrometry indicated that BSA could enhance the fluorescence intensity of EHC by forming a 1:1 EHC-BSA fluorescent complex through static mechanism at pH 4.70 and 7.40 respectively. Furthermore, EHC bound on site 1 in BSA.

Key Words : 3,3',3'',3'''-Ethylenetetraakis-4-hydroxycoumarin (EHC), Bovine serum albumin (BSA), Interaction, Spectrometry

Introduction

3,3',3'',3'''-Ethylenetetraakis-4-hydroxycoumarin (EHC, Fig. 1), a human immunodeficiency virus type1(HIV-1) reverse transcriptase inhibitor, is a novel multi-hydroxyl coumarin compound. At this respect, we research group had reported microwave-induced synthesis of EHC and influence of pH on the spectral properties of EHC.¹ It has to be pointed out, however, there are no detailed research works concerning the interaction between EHC and serum albumins at different pH values till now.

Serum albumins are a group of soluble proteins in human circulatory system which have already been applied to the deposition and transport of many pharmaceutical or bio-active molecules in human blood. Thus, it is significant that whether EHC could be bound to serum albumin and be transported in human blood. And the study of the interaction between EHC and serum albumins is quite useful for the understanding of the binding mechanism as well as providing guidance for the application of new drugs.

In this study, we investigated the interaction of EHC with serum albumins using bovine serum albumin (BSA) as a

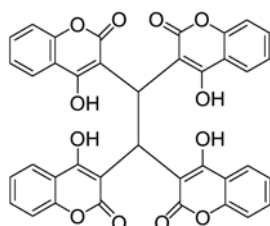


Fig. 1. The structure of EHC.

model protein because of its structural homology with human serum albumin (HSA) and long-standing interest in protein community.² In the consideration of both the isoelectric point of BSA (pH 4.7) and the multi-hydroxyl groups contained in EHC, the interaction of EHC with BSA was established in acetate buffer (pH 4.70) and phosphate buffer (pH 7.40) respectively.

Quite a few investigating methods such as UV-vis absorption,² fluorescence spectrometry³ and electrochemical method⁴ have been applied to the study of the interaction between BSA with pharmaceutical molecules. And more information could be obtained by the combination of these methods. In this paper, we discussed the interaction of EHC with BSA using UV-vis absorption spectrometry and fluorescence spectrometry. The response from each technique was investigated independently and the qualitative and quantitative information offered by each of the methods were compared and analyzed. Detailed information on the interaction between EHC and BSA such as the types of binding force involved in the interaction, the binding constants, the influence of medium conditions on the interaction as well as the effect of EHC on the conformation of BSA were offered in this work. In addition, an original method to deal with the fluorescence enhancement effect according to fluorescence quenching theory was developed in the research work.

Experimental

Materials. All the reagents used were of analytical grade unless otherwise indicated. The water used was twice distilled. BSA was purchased from the Sinopharm Chemical

Reagent Limited Company in Shanghai. All calculations reported for BSA were in terms of BAS with the molecular weight of 67,000. A 1.00×10^{-4} mol·L⁻¹ stock solution of BSA was prepared by directly dissolving the proteins in twice distilled water and stored at 277 K. Pure EHC was obtained from Xi'an University of Architecture and Technology. Its structure was confirmed by Infrared, NMR and Ultraviolet spectroscopy. A stock solution of EHC with the concentration of 1.00×10^{-3} mol·L⁻¹ was obtained by dissolving pure EHC in *N,N*-dimethylformamide (DMF). EHC solution with different pH values were controlled by Britton-Robinson buffer. EHC and/or BSA solution with pH 4.70 and pH 7.40 for later experiments were controlled by 0.1 mol·L⁻¹ acetate buffer and 1/15 mol·L⁻¹ phosphate buffer, respectively.

Instruments. UV-vis absorption spectra were recorded on a Nicolet Evolution 300 UV-visible spectrophotometer with 1.0 cm quartz cells. Fluorescence spectra measurements were performed on a 960MC fluorophotometer equipped with a mercury lamp source and a 1.0 cm quartz cell. The width of the excitation slit was 10 nm. The excitation wavelength was 365 nm.

Procedures. In a series of 10 mL volumetric flasks, 0.30 mL EHC stock solution and different volumes of BSA stock solution were diluted to the mark with acetate buffers (pH 4.70) and phosphate buffers (pH 7.40), respectively. The resulting solutions were allowed to stand for 10 min before analyzed on the UV-visible spectrophotometer in the range of wavelength from 200 to 450 nm. The measurement of 1.00×10^{-6} mol·L⁻¹ BSA solution in the two buffers in the absence and presence of EHC was also performed with the similar procedures.

In a series of 10 mL volumetric flasks, 0.03 mL of EHC solution and different volumes of BSA solution were diluted to the mark with acetate buffer (pH 4.70) and phosphate buffer (pH 7.40), respectively. The solutions obtained were kept still for 10 min, and then analyzed with fluorophotometer.

Results and Discussion

UV-vis Absorption Spectra of EHC and its Binding with BSA. Figure 2 shows the UV-vis absorption spectra of 3.00×10^{-5} mol·L⁻¹ EHC in B-R buffers as a function of pH of the EHC solutions. It could be observed that pH had a large effect on the UV-vis absorption properties of the EHC solutions. And it was demonstrated that there were pronounced pH-dependent structural changes in EHC, which might be related to the protonation or deprotonation of EHC.⁵⁻⁷

Figure 3 gives the UV-vis absorption spectra of 3.00×10^{-5} mol·L⁻¹ EHC in acetate buffer of pH 4.70 in the absence or presence of BSA. The absorption spectra indicated that compared with the absorption of the EHC samples without BSA, after the addition of BSA, the absorption of the samples at 243 nm decreased at first, but then increased with the increase of the amount of BSA in the sample solutions,

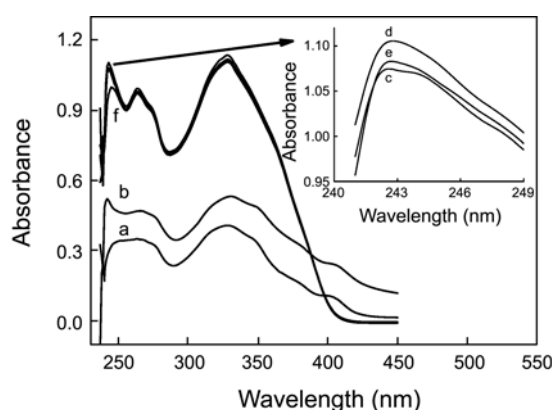


Fig. 2. The absorption spectra of 3.00×10^{-5} mol·L⁻¹ EHC in B-R buffers as a function of pH. (a) 2.10; (b) 3.20; (c) 4.70; (d) 5.90; (e) 7.40; (f) 9.20.

whereas the absorption of the samples at 264 nm increased gradually with the addition of the concentration of BSA in the samples.

As shown in Figure 3, the absorption at 329 nm resulted from the conjugated system composed of carbonyl group and benzene ring which formed after the protonation of ester group's oxygen⁸ in EHC. With the increase of BSA, this absorption decreased with the bathochromic shift of its absorption band. From this it could be deduced that the energy level of the conjugated system changed because of the interaction of either carbonyl or hydroxyl of EHC with BSA.⁷

In addition, Figure 3 demonstrated that with the increase of the concentration of BSA in the EHC contained samples, large wavelength hypsochromic shifted and hyperchromic effect appeared. Furthermore, an isosbestic point at 292 nm was observed. These changes in the absorption spectra implied that there were intensive binding interactions between EHC and BSA, and that a new EHC-BSA complex has been formed.

The binding constant K_A of EHC with BSA was calculated

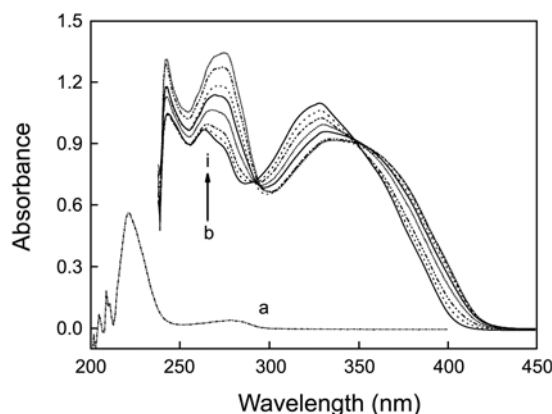


Fig. 3. Absorption spectra of 10.00×10^{-6} mol·L⁻¹ BSA (a) and 3.00×10^{-5} mol·L⁻¹ EHC in the absence (b) as well as presence [(c)-(i)] of different concentrations of BSA (10^{-6} mol·L⁻¹): (c): 1.00; (d): 3.00; (e) 4.00; (f) 6.00; (g) 8.00; (h) 10.00; (i): 12.00 at pH 4.70.

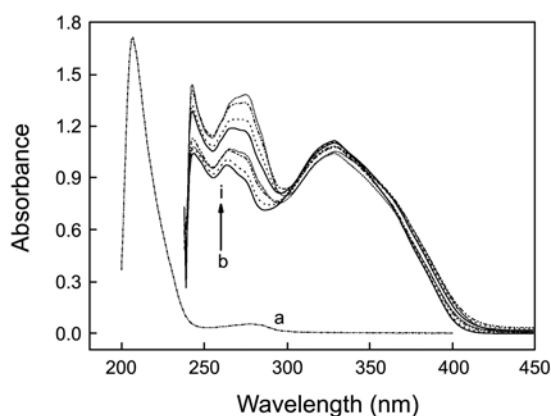


Fig. 4. Absorption spectra of $10.00 \times 10^{-6} \text{ mol}\cdot\text{L}^{-1}$ BSA (a) and $3.00 \times 10^{-5} \text{ mol}\cdot\text{L}^{-1}$ EHC in the absence (b) as well as presence [(c)-(i)] of different concentrations of BSA ($10^{-6} \text{ mol}\cdot\text{L}^{-1}$): (c): 1.00; (d): 3.00; (e): 4.00; (f): 6.00; (g): 8.00; (h): 10.00; (i): 12.00 at pH 7.40.

by the Lineweaver-Burk equation by the data from UV-vis measurement⁹:

$$(A-A_0)^{-1} = A_0^{-1} + K_A^{-1}A_0^{-1}[Q]^{-1} \quad (1)$$

Where K_A is the binding constant, which can be calculated by the ratio of intercept and slope, A_0 and A are the absorbance of EHC in the absence and presence of BSA. From the absorbance of EHC at 264 nm which changed regularly relatively, the linear equation of Lineweaver-Burk was fitted as $(A-A_0)^{-1} = -0.6883 + 5.502[10^5 C_{\text{BSA}}]^{-1}$ ($r = 0.9934$), yielding a binding constant of $1.250 \times 10^4 \text{ L}\cdot\text{mol}^{-1}$ at 291 K.

Figure 4 gives the UV-vis absorption spectra of $3.00 \times 10^{-5} \text{ mol}\cdot\text{L}^{-1}$ EHC in phosphate buffer of pH 7.40. It could be observed that the absorption spectra of EHC in the absence or presence of BSA in phosphate buffer were different from corresponding absorption spectra in acetate buffer, as was shown in Figure 3. For samples in phosphate buffer, after the addition of BSA, these samples still showed absorption peak at 329 nm as the EHC sample without BSA, but the absorption intensity decreased a little (Fig. 4). It might be concluded that the energy level of the conjugated system of EHC and BSA did not change obviously. Meanwhile, for the samples in phosphate buffer with BSA, large wavelength hypsochromic shift, hyperchromic effect and an isosbestic point at 295 nm were observed implying the formation of a new EHC-BSA complex.

The data collected from UV-vis absorption spectra of EHC samples in phosphate buffer were calculated by using the similar method applied to relative data of EHC samples in acetate buffer. The linear plot of Lineweaver-Burk equation was fitted as $(A-A_0)^{-1} = 0.3506 + 3.119 [10^5 C_{\text{BSA}}]^{-1}$ ($r = 0.9981$), yielding a binding constant of $1.124 \times 10^4 \text{ L}\cdot\text{mol}^{-1}$ at simulative physiological condition.

UV-vis Absorption Spectra of BSA in the Presence of EHC. To obtain information on the interaction of EHC with BSA from different aspects, we further studied the effect of EHC on UV-vis absorption spectra of BSA at two media as

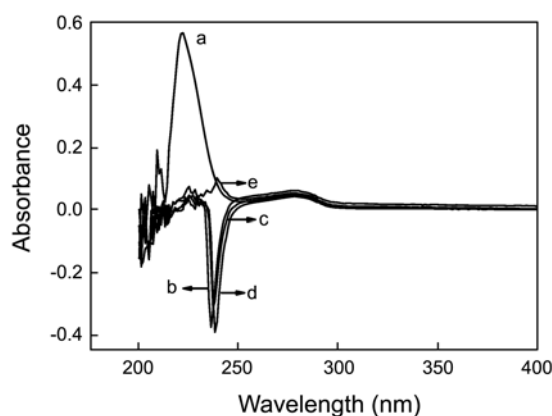


Fig. 5. Absorption spectra of $1.00 \times 10^{-6} \text{ mol}\cdot\text{L}^{-1}$ BSA after addition of EHC ($\times 10^{-7} \text{ mol}\cdot\text{L}^{-1}$): (a) 0; (b) 0.50; (c) 0.80; (d) 1.00; (e) 1.50; pH = 4.70.

mentioned above.

As was shown in Figure 5, for BSA samples without EHC, the absorption at 222 nm evoked by C=O transition with $\pi-\pi^*$ represented the helix structure of BSA.¹⁰ The absorption of BSA at 278 nm represented both indole ring of tryptophan residue and benzene ring of tyrosine residue transition with $\pi-\pi^*$.¹¹ By contrast, with the addition of EHC, the absorption peak at 222 nm disappeared but a negative peak next to 235 nm appeared. This phenomenon might arise from the formation of hydrogen bonds between the oxygen-containing groups in EHC and amino group or carbonyl group of amino acid residue in BSA. As a result, the bond intension of amino group or carbonyl group was weakened, leading to the decrease of absorbance and bathochromic shift of absorption band.¹² On the other hand, after the addition of EHC, the BSA samples still showed absorption peak at 278 nm as the sample without EHC. But the absorbance intensity at 278 nm changed. This proved that after the addition of EHC, the extent of peptide chain in BSA has changed, which induced bareness extent changes of both tryptophan residue and tyrosine residue.¹³

In the phosphate buffer of pH 7.40, EHC had similar effect on UV-vis absorption spectra of the BSA samples as on the

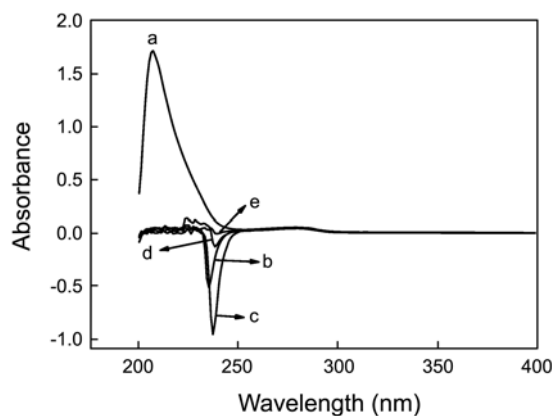


Fig. 6. Absorption spectra of $1.00 \times 10^{-6} \text{ mol}\cdot\text{L}^{-1}$ BSA after addition of EHC ($\times 10^{-7} \text{ mol}\cdot\text{L}^{-1}$): (a) 0; (b) 0.50; (c) 0.80; (d) 1.00; (e) 1.50; pH = 7.40.

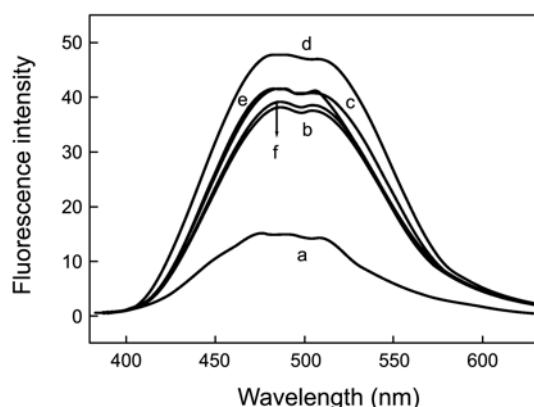


Fig. 7. The fluorescence spectra of $3.00 \times 10^{-6} \text{ mol}\cdot\text{L}^{-1}$ EHC at different pHs: (a) 2.10; (b) 3.20; (c) 4.70; (d) 5.90; (e) 7.40; (f) 9.20.

absorption of BSA samples in acetate buffer of 4.70. As shown in Figure 6, in phosphate buffer, with the addition of EHC, the changes of absorption band of BSA at 207 nm indicated that hydrogen bond was involved in the interaction of EHC with BSA, the same as in the corresponding interaction in pH 4.70 medium. But different from BSA samples in the acetate buffer, the absorption peak of BSA at 278 nm didn't change after the addition of EHC in pH 7.40 phosphate medium, which meant that the extent of peptide chain in BSA kept constant.

Fluorescence Spectra of EHC in B-R Buffers and in pH 4.70 Acetate Buffer. Figure 7 presents the fluorescence spectra of EHC at different pH in B-R buffers. It was indicated that pH of the EHC-containing samples had noticeable effect on the fluorescence spectra of these samples. And similar to the influence of pH on UV-vis spectra of EHC samples, the fluorescence spectra of EHC reached maximum intensity at pH 5.90.

Figure 8 exhibits the emission spectra of EHC with or without BSA in pH 4.70 acetate buffer. Compared with the sample without BSA, the increase of fluorescence intensity and the maximum wavelength hypsochromic shift were

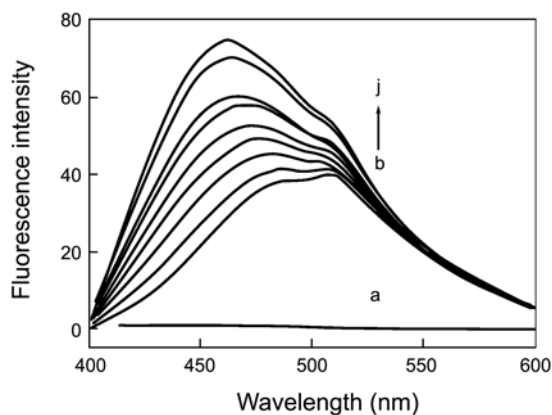


Fig. 8. Fluorescence spectra of $1.80 \times 10^{-6} \text{ mol}\cdot\text{L}^{-1}$ BSA (a) and $3.00 \times 10^{-6} \text{ mol}\cdot\text{L}^{-1}$ EHC with different concentrations of BSA. C_{BSA} from b to j: 0, 0.20, 0.40, 0.60, 0.80, 1.00, 1.20, 1.50 and 1.80 ($\times 10^{-6} \text{ mol}\cdot\text{L}^{-1}$); pH = 4.70.

observed after the addition of BSA. The reason for these changes was that BSA caused the concentration-dependent enhancement of the intrinsic fluorescence of EHC. These results indicated that there were strong interactions between EHC and BSA.³

The mechanism of fluorescence enhancement: In order to confirm the enhancement mechanism, the fluorescence data at different temperatures was analyzed with the well-known Stern-Volmer equation and Lineweaver-Burk equation, which were commonly used in describing dynamic quenching and static quenching, respectively. In this paper, these two equations were used to describe the fluorescence enhancement mechanism.

The Stern-Volmer equation is as follows¹⁴:

$$F/F_0 = 1 + K_{\text{SV}} [Q] \quad (2)$$

Where K_{SV} is the Stern-Volmer enhancement constant with the unit of $\text{L}\cdot\text{mol}^{-1}$, $[Q]$ is the concentration of the enhancer (BSA). Lineweaver-Burk equation is shown below as equation 3¹⁵:

$$(F-F_0)^{-1} = F_0^{-1} + K_{\text{LB}}^{-1} F_0^{-1} [Q]^{-1} \quad (3)$$

Where K_{LB} is the static enhancement constant with the unit of $\text{L}\cdot\text{mol}^{-1}$, which describes the binding efficiency of micro-molecules to biological macromolecules at ground state. The data collected from fluorescence enhancement spectra at two different temperatures were disposed of

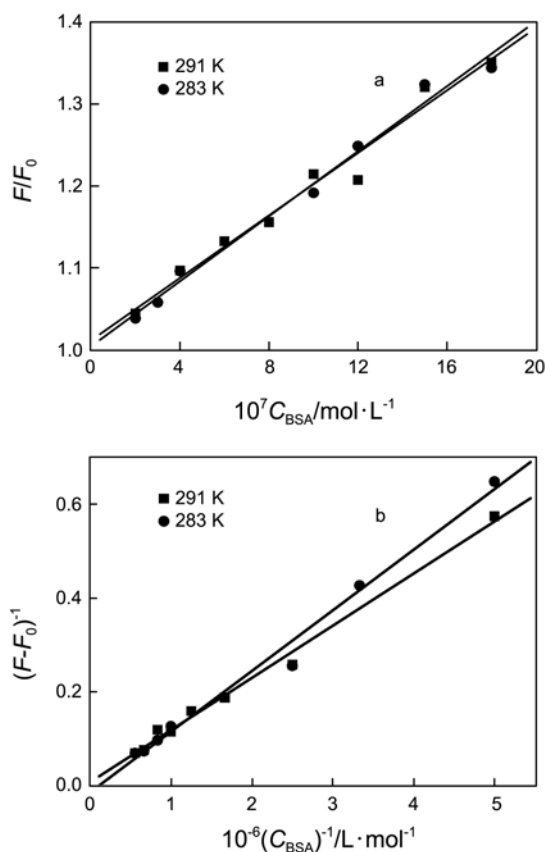


Fig. 9. The Stern-Volmer (a) and Lineweaver-Burk (b) curves at different temperatures. $C_{\text{EHC}} = 3.00 \times 10^{-6} \text{ mol}\cdot\text{L}^{-1}$.

Table 1. Regression equations and correlation coefficient r of EHC's binding to BSA. pH = 4.70

T/K	regression equation	r
291	$F/F_0 = 1.011 + 0.01911 \times 10^7 C_{\text{BSA}}$	0.9871
283	$F/F_0 = 1.004 + 0.01987 \times 10^7 C_{\text{BSA}}$	0.9938
291	$(F-F_0)^{-1} = 0.00958 + 0.1108 \times 10^{-6} C_{\text{BSA}}^{-1}$	0.9962
283	$(F-F_0)^{-1} = -0.01198 + 0.1288 \times 10^{-6} C_{\text{BSA}}^{-1}$	0.9940

according to Eq. (2) and Eq. (3), respectively, as shown in Figure 9. The equations and their correlation coefficients were shown in Table 1.

From Figure 9 and Table 1, it could be seen that the curves of Lineweaver-Burk equation had better linear relations than Stern-Volmer equation. It was obvious that the enhancement process was largely related to static process.¹⁶ Meanwhile, the fact, that the absorption spectra of EHC-BSA system (Fig. 3) were different from those of lonely BSA or lonely EHC, also confirmed that at least one EHC-BSA complex with certain new structure had been formed. Consequently, a conclusion might be safely drawn that the enhancement of the BSA-EHC system belonged to static enhancement with complex formation.¹⁷

As discussed above, the enhancement had been proved to originate from the formation of the complex but not be initiated by dynamic collision. When small molecules bound independently to a set of equivalent sites on the macromolecule,¹⁸ the equilibrium between free and bound molecules could be given by the following equation¹⁹:

$$\log[(F-F_0)/F] = \log K_A + n \log [Q] \quad (4)$$

K_A is the apparent binding constant to a site and n is the number of binding sites per BSA. The dependence of $\log [(F-F_0)/F]$ on the value of $\log [Q]$ is linear with slope equal to the value of n , and the value $\log K_A$ is fixed on the ordinate. The data from two different temperatures was handled in this way and consequently we obtained the following equations $\log[(F-F_0)/F] = 4.074 + 0.80871 \log C_{\text{BSA}}$ (291 K) ($r = 0.9915$), and $\log[(F-F_0)/F] = 4.535 + 0.8864 \log C_{\text{BSA}}$ (283 K) ($r = 0.9932$), which suggested that the assumptions underlying the derivation of Eq. (4) were satisfactory. Therefore, the values of K_A were calculated to be 1.186×10^4 (291 K) and $3.428 \times 10^4 \text{ L} \cdot \text{mol}^{-1}$ (283 K). In addition, n was calculated to be 0.8. These results implied that EHC could be bound to BSA efficiently and the binding process involved only one binding site.

It is universally acknowledged that there are two typical binding sites in BSA, site I and site II, which are usually located in IIA and IIIA structural field of BSA, respectively.

The drugs bound to BSA on site I are generally bulky heterocyclic anions with the charge situated in a central position of the molecules, and the drugs bound on site II are aromatic carboxylic acids with an extended conformation and the negative charge located at one end of the molecule.^{20,21} EHC molecule contains large conjugated systems and its charges are located in the ring of the conjugated system. From the calculation above we could know that

there was about one binding site. So EHC binds on site I in BSA,²² which was consistent with other literature.²³ In addition, the crystal structure of human serum albumin (HSA) in complex with thyroxine (3,3',5,5'-tetraiodo-L-thyroxine) was downloaded from the protein data bank, with amino acids matching method to predict residues of BSA for Site I and Site II. Ehits program was applied to calculate the interaction mode between EHC and HSA. We concluded that EHC could interact with HSA at site I, and the interaction between EHC and HSA was dominated by Van-der-Waals force and hydrophobic force. Therefore, we could draw the prediction that EHC bound on site I in BSA, not the other site II of BSA.

Thermodynamic Parameters and Nature of Binding Force. The interaction forces between drug molecules and biomolecules may involve hydrophobic force, electrostatic interactions, van der Waals interactions and hydrogen bond, etc. In order to elucidate the interaction forces of EHC with BSA, the thermodynamic parameters were calculated according to Eqs. (5)-(7). If the temperature (T) did not vary significantly, the enthalpy change (ΔH) could be regarded as a constant. The free energy change (ΔG) could be estimated from the following equation, which was based on the binding constants at different temperatures. ΔH and entropy change (ΔS) could be calculated from the following equations:

$$\Delta G = \Delta H - T \cdot \Delta S \quad (5)$$

$$\Delta G = -RT \ln K_A \quad (6)$$

$$\ln(K_2/K_1) = (\Delta H/R) \cdot (1/T_1 - 1/T_2) \quad (7)$$

Where R is the gas constant and K_A is the binding constant at the corresponding temperature (T). Table 2 shows the values of ΔH , ΔS and ΔG . The negative sign for ΔG indicated that an automatic reaction happened between EHC and BSA. The negative ΔH and ΔS values revealed that hydrogen bond and van der Waals force played a major role in the binding of EHC to BSA.²⁴

Fluorescence Spectra of EHC in Phosphate Buffer of pH 7.40. Figure 10 presents the emission spectra of EHC in the absence and presence of BSA in phosphate buffer of pH 7.40. The similar phenomenon was observed as the emission spectra of EHC in acetate buffer of pH 4.70. After the addition of BSA, changes of both fluorescence and the maximum wavelength of EHC were also observed, which implied that there were interactions between EHC and BSA. The equations of Stern-Volmer, Lineweaver-Burk and their correlation coefficients at different temperatures were calculated and shown in Table 3. From Table 3 and Figure 4, it could be deduced that the enhancement was in agreement with the static process.

Table 2. The binding constant of EHC with BSA and the thermodynamic parameters. pH = 4.70

T/K	$K_A/\text{L} \cdot \text{mol}^{-1}$	$\Delta H/\text{KJ} \cdot \text{mol}^{-1}$	$\Delta S/\text{J} \cdot \text{mol}^{-1} \cdot \text{K}^{-1}$	$\Delta G/\text{KJ} \cdot \text{mol}^{-1}$
291	1.186×10^4	-98.10	-259.11	-22.70
283	3.428×10^4	-98.10	-259.82	-24.57

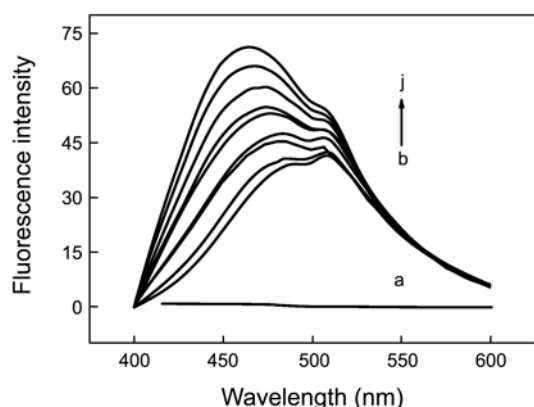


Fig. 10. Fluorescence spectra of $1.80 \times 10^{-6} \text{ mol}\cdot\text{L}^{-1}$ BSA (a) and $3.00 \times 10^{-6} \text{ mol}\cdot\text{L}^{-1}$ EHC with different concentrations of BSA. C_{BSA} from b to j: 0, 0.20, 0.40, 0.60, 0.80, 1.00, 1.20, 1.50 and $1.80 (\times 10^{-6} \text{ mol}\cdot\text{L}^{-1})$; pH = 7.40.

Table 3. Regression equations and correlation coefficient r of EHC's binding to BSA. pH = 7.40

T/K	Regression equation	r
291	$F/F_0 = 1.018 + 0.01527 \times 10^7 C_{\text{BSA}}$	0.9900
283	$F/F_0 = 1.014 + 0.01182 \times 10^7 C_{\text{BSA}}$	0.9908
291	$(F-F_0)^{-1} = 0.00976 + 0.1265 \times 10^{-6} C_{\text{BSA}}^{-1}$	0.9991
283	$(F-F_0)^{-1} = 0.02244 + 0.1534 \times 10^{-6} C_{\text{BSA}}^{-1}$	0.9979

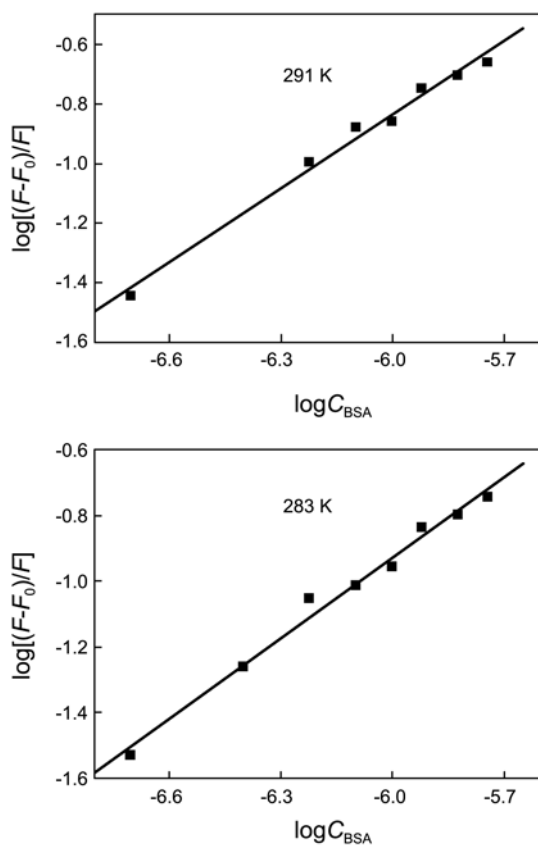


Fig. 11. Plots of $\log[(F-F_0)/F]$ vs. $\log C_{\text{BSA}}$ of EHC-BSA. $C_{\text{EHC}} = 3.00 \times 10^{-6} \text{ mol}\cdot\text{L}^{-1}$; pH = 7.40.

Table 4. The binding constant of EHC with BSA and the thermodynamic parameters. pH = 7.40

T/K	$K_A/\text{L}\cdot\text{mol}^{-1}$	$\Delta H/\text{KJ}\cdot\text{mol}^{-1}$	$\Delta S/\text{J}\cdot\text{mol}^{-1}\cdot\text{K}^{-1}$	$\Delta G/\text{KJ}\cdot\text{mol}^{-1}$
291	1.418×10^4	32.58	191.4	-23.13
283	9.964×10^3	32.58	191.7	-21.66

The binding equilibrium equations at two different temperatures were listed in Figure 11, from which the equation $\log[(F-F_0)/F] = 4.152 + 0.8314\log[C_{\text{BSA}}]$ (291 K) ($r = 0.9937$) and $\log[(F-F_0)/F] = 3.998 + 0.8214\log[C_{\text{BSA}}]$ (283 K) ($r = 0.9932$) were obtained. Therefore, the values of K_A were calculated to be 1.418×10^4 (291 K) and $9.964 \times 10^3 \text{ L}\cdot\text{mol}^{-1}$ (283 K). From the data n ($n \approx 1$), it could be inferred that for the interaction between EHC and BSA, there was only one independent class of binding site on BSA, the same as for the corresponding interaction in acidic solution.

As listed in Table 4, the sign of ΔG was negative which meant that the process of the interaction between EHC and BSA took place spontaneously in pH 7.40 phosphate buffer. The positive values of ΔH and ΔS implied that hydrophobic force played a major role in the binding of EHC to BSA.²⁴ All these indicated that the interaction might proceed through the aromatic rings of EHC and the BSA molecules.

Conclusion

In this paper, the interaction of EHC with BSA was investigated by UV-vis absorption spectrometry and fluorescence spectrometry. The results presented clearly that the binding of EHC to BSA was related to the pH value of medium which resulted in different existing states of both EHC and BSA. Different interaction forces involved in the interaction of the two molecules were deduced. The methods proposed for the analysis of the interaction were effective, rapid and low cost. And the result of the application of fluorescence quenching theory to fluorescence enhancement was satisfactory. In addition, the fact that the EHC-BSA possesses large binding constant (K_A) at two different pHs proved that there were strong interactions between EHC and BSA. It might be deduced that EHC was deposited and transported by albumin. These studies contributed to the understanding of the antiviral activity of EHC-an important AIDs drug.

Acknowledgments. The authors appreciate the support from the National Natural Science Foundation of China (No. 50830303), the Education Department Foundation of Shaanxi Province in China (No. 11JK0570) and the Research Achievements Foundation of Xian University of Architecture and Technology (No. ZC1004).

References

- Dong, S. Y.; Li, J.; Huang, T. L. *Chem. J. Chinese Universities* **2009**, *30*, 1516.
- Xu, H.; Liu, Q. W.; Wen, Y. Q. *Spectrochim. Acta A* **2008**, *71*, 984.

3. Liu, X. H.; Xi, P. X.; Chen, F. J.; Xu, Z. H.; Zeng, Z. Z. *J. Photochem. Photobiol. B: Biol.* **2008**, *92*, 98.
 4. Li, Y. Q.; Guo, Y. J.; Li, X. F.; Pan, J. H. *Talanta* **2007**, *71*, 123.
 5. Liu, C. G.; Xu, Y. Z.; Wei, Y. J.; Zhao, J.; Q, J.; Wang, X. H.; Xu, Z. H.; Wu, J. G. *Spectros. Spect. Anal.* **2005**, *25*, 1446.
 6. Du, L. M.; Jin, W. J.; Dong, C.; Liu, C. S. *Spectros. Spect. Anal.* **2001**, *21*, 518.
 7. Xie, M. X.; Xu, X. Y.; Wang, Y. D.; Liu, Y. *Acta Chim. Sin.* **2005**, *63*, 2055.
 8. Zhu, M. H. "Instrument Analysis", High Education Press, Bei Jing, **2000**, 281.
 9. Liu, Y.; Xie, M. X.; Kang, J. *Acta Chim. Sin.* **2003**, *61*, 1305.
 10. Shahid, F.; Gomez, J. E.; Birnbaum, E. R.; Darnall, D. W. *J. Biochem.* **1982**, *257*, 5618.
 11. Wei, X. F.; Ding, X. M.; Liu, H. Z. *Spectros. Spect. Anal.* **2004**, *20*, 556.
 12. Feng, Y. Y.; Wu, X. H.; Zhou, J. H.; Gu, X. T.; Lu, T. H.; Wang, X. S.; Zhang, B. W. *Chin. J. Appl. Chem.* **2005**, *22*, 895.
 13. Li, X. J.; Wang, Z. Q.; Chen, J.; Zhang, S. G. *Chin. J. Appl. Chem.* **1998**, *15*, 5.
 14. Sułkowska, A.; Równicka, J.; Bojko, B. Sułkowska, W. *J. Mol. Struct.* **2003**, *133*, 651.
 15. Zhang, H. X.; Huang, X.; Mei, P.; Gao, S. *J. solution Chem.* **2008**, *37*, 631.
 16. Deng, S. X.; Yang, J. D. *J. Anal. Sci.* **2007**, *23*, 177.
 17. Zhang, H. X.; Mei, P.; Yang, X. X. *Spectrochim. Acta A* **2009**, *72*, 621.
 18. Shaikh, S. M. T.; Seetharamappa, J.; Ashoka, S.; Kandaga, P. B. *Dyes Pigments* **2007**, *73*, 211.
 19. Hu, Y. J.; Li, W.; Liu, Y.; Dong, J. X.; Qu, S. S. *J. Pharm. Biomed. Anal.* **2005**, *39*, 740.
 20. Dockal, M.; Chang, M.; Carter, D. C.; Rüker, F. *Protein. Sci.* **2000**, *9*, 1455.
 21. Peters, T. J. *All About Albumin: Biochemistry Genetics and Medical Applications*; Academic Press: Inc., New York, 1996.
 22. Xie, M. X.; Xu, X. Y.; Wang, Y. D. *Biochim. Biophys. Acta* **2005**, *1724*, 215.
 23. He, X. M.; Carter, D. C. *Nature* **1992**, *358*, 209.
 24. Ross, P. D.; Subramanian, S. *Biochem.* **1981**, *20*, 3096.
-